Available online at www.sciencedirect.com
SCIENCE DIRECT
ELSEVIER
Icarus 171 (2004) 516–524
ICARUS
www.elsevier.com/locate/icarus

The edge of the Kuiper belt: the Planet X scenario

M.D. Melita [a,*], I.P. Williams [a], Simon J. Collander-Brown [b], Alan Fitzsimmons [b]

[a] *Astronomy Unit, School of Mathematical Sciences, Queen Mary, University of London, Mile End Rd., London E1 4NS, UK*
[b] *School of Maths and Physics, APS Division, Queens University Belfast, Belfast BT7 1PX, UK*

Received 23 April 2003; revised 7 May 2004

Available online 29 July 2004

Abstract

Our goal is to determine whether or not the observed sudden termination of the Edgeworth–Kuiper belt can be the result of perturbations from a hypothetical planet. We investigate the effects that such an object would produce on the primordial orbital distribution if the trans-neptunian objects, for a range of masses and orbital parameters of the hypothetical planet. In this numerical investigation, the motion of the hypothetical planet was influenced by the existing planets but not by its interaction with the disk. We find that no set of parameters produce results that match the observed data. Dynamical interaction with the disk is likely to be important so that the orbit of the hypothetical planet changes significantly during the integration interval. This is also discussed. The overall conclusion is that none of the models for the hypothetical planet that were investigated can reproduce the observed features of the Edgeworth–Kuiper belt starting from any probable primordial distribution.

Keywords: Trans-neptunian objects; Planetary dynamics; Orbits; Origin, solar system

1. Introduction

Since the discovery by Jewitt and Luu (1993) of the first trans-neptunian object the region has proved to be full of unexpected features (see Fig. 1). First, it was realized that a large number of the objects were orbiting in mean-motion resonances with Neptune, most residing in the 2 : 3 exterior mean-motion resonance. Because their orbits are similar to that of Pluto, these members are popularly known as plutinos. As the number of plutinos initially appeared to be very high compared to what might be expected from random capture, Malhotra (1995) suggested that radial migration of Neptune could enhance the number of objects captured in resonance. However, recent observations by Trujillo et al. (2001) indicate that the ratio of the number of known resonant to classical Edgeworth–Kuiper objects (EKOs) do not show an excess of the former, which either removes the need for the radial migration hypothesis or implies that the capture efficiency is smaller than previously suggested (Melita and Brunini, 2000). An additional subclass of EKO's has now been identified, composed of objects moving on orbits with large semimajor axes and high eccentricity. They have popularly been called the 'Scattered disk objects' (SDOs), because it was considered that they formed as a result of recurrent close encounters of classical belt objects with Neptune (Duncan and Levison, 1997). However, the discovery of some SDOs with perihelia so large as to be beyond the control of the Neptune has led to other theories for their origin (Gladman et al., 2001; Collander-Brown et al., 2001).

As more EKOs were discovered and the distribution of orbital elements became gradually known, it was realized that there were many more objects on orbits with high eccentricity and high inclination than might be expected on a formation model within a standard solar nebula. A number of explanations for this have been suggested, including a transient interaction with a massive planetesimals (Morbidelli and Valsechi, 1997), secular-resonance sweeping (Nagasawa and Ida, 2000; Gomes, 2003) and a close stellar passage (Ida et al., 2000).

It is also clear that beyond 50 AU there is a total lack of discoveries of trans-neptunian objects with low eccentricities and inclinations. There is an edge to the classical Edgeworth–Kuiper belt (Trujillo and Brown, 2001; Allen et

* Corresponding author.
E-mail address: m.d.melita@qmul.ac.uk (M.D. Melita).

0019-1035/$ – see front matter
doi:10.1016/j.icarus.2004.05.014

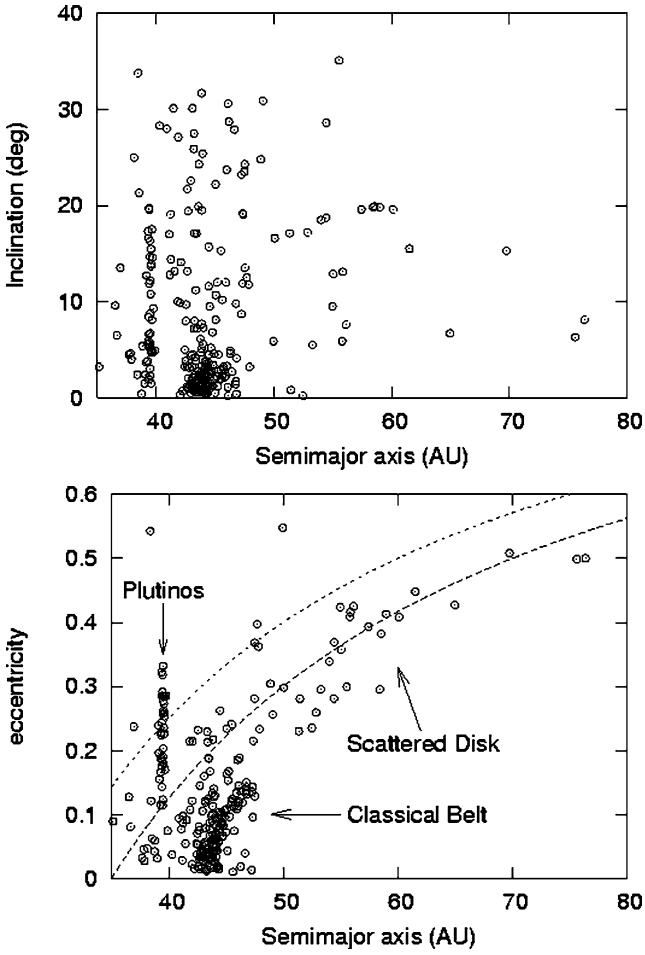

Fig. 1. Observed multiopposition EKBOs. The lines of perihelion distance at 30 and 35 AU are indicated.

al., 2001). It was suggested by Stern and Colwell (1997a) that at large distances the relative velocities are too small for self-interactions to be important, so that an increase of the EKO surface density should be expected beyond 50 AU. Present observations indicate that, if the edge at 50 AU represents the start of a gap rather than the termination of the disk, then the 'outer' disk does not start again until at least ~ 75 AU from the Sun. Levison and Morbidelli (2003) suggested that these features can be explained if the belt initially formed closer to the Sun and was pushed outwards as a consequence of the outward migration of Neptune.

Another possible explanation for both the highly excited state and the edge is the existence of some other perturbing agent, not yet included in dynamical theory, which operated—or operates—in the region. Two possibilities are either a close stellar passage or an undiscovered planet. The stellar passage scenario has been discussed (Ida et al., 2000; Kobayashi et al., 2004; Melita et al., 2004). In this work we investigate the plausibility of the additional planet hypothesis. It is clear, as was shown by Brunini and Melita (2002) that a Mars-sized body orbiting at ~ 60 AU at a moderately eccentric and inclined orbit can provide the perturbations necessary to remove objects from that general location. What has not been investigated is whether such a body can also generate high inclination high eccentricity orbits while preserving the numbers of resonant and classical bodies. We thus investigate numerically the effects of a hypothetical planet (with various masses and orbital parameters) on the distribution of bodies in the Edgeworth–Kuiper belt.

2. The dynamics of the classical EKB–Planet X interaction

A broad-brush view of the effects of a tenth planet is easy to describe. The observed classical Edgeworth–Kuiper objects lie on orbits that are far from Neptune. Hence, except for those lying close to a secular resonance (for the location of secular resonances see Knezévic et al., 1991), their orbits are stable (Duncan et al., 1995). On the other hand, because of their high eccentricity, the scattered belt objects can have perihelia close to the orbit of Neptune and their orbits can be heavily perturbed in a close encounter. Since slightly different geometries of the close encounter can result in very different outcomes, the scattering can be regarded as chaotic. The end-states could range from Centaurs to objects in hyperbolic orbits (Levison and Duncan, 1997).

Planet X perturbs the surrounding objects mainly through gravitational close encounters, which is an interaction with a timescale much smaller than the orbital period. For a thin disk, the period between encounters depends on the synodic period. The strength of the perturbation depends on the semimajor axis, the relative longitudes and the mass of Planet X (see, for example, Duncan et al., 1989). Subsequent to each encounter, the interaction with Planet X is negligible, unless the objects fall into any of its resonances.

If the initial eccentricity of the EKBO is large, it can be reduced following an encounter. Thus, with time, in an a–e plot a bell-shaped distribution develops, centered at the semimajor axis of the Planet X. Objects with large synodic period compared to that of Planet X suffer encounters only rarely. How sharp and tall the bell distribution is depends on the mass and orbit of Planet X.

3. The model

It is clear that the dynamics described above can not be followed by analytical means. Our simulations involve the numerical integration of the equations of motion of massless particles representing the primordial Edgeworth–Kuiper belt in the region of interest. These are assumed to move through the gravitational field of the Sun, the four giant planets and Planet X, of roughly terrestrial size. Planet X is assigned sets of differing initial values of semimajor axis, a_P, eccentricity e_P, inclination i_P and mass m_P. Other than the effects of the Sun and the four major planets, no other perturbations are considered to act on Planet X in this simulation. Hence

there is little change in the orbital parameters of Planet X throughout the simulation.

A total of 300 bodies were taken to represent the initial belt, with orbital elements uniformly distributed in the ranges $35 < a < 80$ AU, $0.0 < e < 0.05$, $0.0° < i < 5.0°$, where a denote the semimajor axis, e the eccentricity and i the inclination. A 'Plutino' population of another 20 test-particles in known long term stable orbits has been also added. We use the stability of this group as an additional constraint.

The numerical integrator used is a hybrid symplectic second order method previously used in Brunini and Melita (2002), which treats close encounters using a Burlish and Stoer integrator with the strategy developed by Chambers (1999). The integration time was in the range of 1–4.5×10^9 years.

Table 1
Initial orbital parameters and masses of the planetoid for each simulation

Run	m_P ($M_\oplus$)	a_P (AU)	e_P	i_P (deg)	$T_{\rm sim}$ (10^9 y)	$f_{\rm PLU}$
1	1/10	56	0.15	10	1	0.5
2	1	60	0.1	10	1	0.65
3	1/3	60	0.2	10	4.5	0.15
4	1/3	60	0.15	10	4.5	0.65
5	1/3	60	0.15	15	4.5	0.45
6	0.2	60	0.2	10	1	0.3
7	1/10	60	0.0	10	1	1
8	1/10	60	0.1	10	1	1
9	1/10	60	0.2	10	1	0.75
10	1/10	60	0.3	10	1	0.2
11	1/10	61	0.2	10	1	0.65
12	0.087	61	0.2	10	4.5	0.6
13	0.16	61	0.2	10	4.5	0.3
14	3.33	70	0.25	10	4.5	0.05

The corresponding total simulated time, $T_{\rm sim}$ and the fraction of plutinos left at the end of the simulation, $f_{\rm PLU}$, are also given.

4. Results

The observed EKB distribution is shown in Fig. 1. The aim of any simulation must be to reproduce something akin to this. In particular we are looking for the continued existence of high eccentricity plutinos, the sharp edge at ~ 48 AU and the existence of SDOs, that is high inclination, high eccentricity objects. There are constraints on the range of values for some of the parameters.

The IRAS survey detected no planet and so the brightness of any hypothetical planet in the infrared must be below the limiting magnitude of that survey. The observed brightness depends on size and distance. Since the infrared brightness comes from emission (rather than reflection), then the results are not sensitive to the albedo. According to Hogg et al. (1991), the maximum allowed mass at 60 AU is about $M_\oplus$, increasing to about $3M_\oplus$ at 70 AU. In our investigations we thus only select masses for Planet X that are consistent with these limits.

A further restriction comes from the fact that a significant number of both plutinos and classical EKBO's must survive. By running our program, we found that planets at 55 AU or less tend to clear completely the EKB. Hence we have not investigate hypothetical planets with a semimajor axis smaller than 55 AU.

A total of 14 runs were carried out, each with a different set of parameters for Planet X. These were not all preselected, the information gleaned from one set of runs was then used to restrict the choice of further sets of parameters. Al runs were inspected after running for 10^9 years. If it was very clear that no serious evolution towards the observed end state was taking place, or that most objects were being lost, the run was terminated. Otherwise the integration continued up to 4.5×10^9 years. The adopted values and integration time are shown in Table 1. The order in the table is by increasing a_P, and not the chronological order in which the runs were actually performed. Also shown in the table is $f_{\rm PLU}$, the fraction of plutinos surviving to the end of the simulation. A small value would indicate that the model is unacceptable, irrespective of its success in generating a gap at 50 AU or a good population of SDO's.

In Fig. 2 we show the final EKB distributions for three different values of the eccentricity of the planetoid, keeping other parameters the same. These are runs 8, 9, and 10 in the above table. It is apparent that high values of both eccentricity and inclination have been generated in all three cases. However, neither the eccentricity nor the inclinations have reached the maximum values in the observed data (Fig. 1) when the eccentricity is 0.1. For the other two values, the eccentricity reaches the correct range, but the inclinations are still low. However, in none of the cases is there any real indication of an edge developing at 50 AU. Hence we conclude that these sets of parameters do not satisfy the requirements. It is also clear that the distribution obtained when $e_P = 0.3$ is no better than that obtained when $e_P = 0.2$. Hence exploration of sets with larger values of e_P was not undertaken. In run 11 (not shown) the semimajor axis was increased slightly to 61 AU, from the value of 60 in run 9, but this did not produce any improvement and so exploration of the parameter space with further small changes in a_P was not undertaken.

In Fig. 3 we investigate the effect of changing the mass of Planet X and show the final distribution for runs 3, 6, and 9, that is with $a_P = 60$ AU, $e_P = 0.2$ and $i_P = 10°$. As expected, there is evidence that increasing the mass increases both the inclination and the eccentricity of the belt population. Indeed it may be claimed that the high end roughly matches the observation. However, there is still no real sign of a gap being cleared or an edge developing.

The major problem in the above runs has been an inability to generate a gap in the final distribution. We thus investigate a set of situations that is most likely to produce a gap, namely an orbit with a perihelion distance close to 50 AU, and a mass as large as possible, consistent with nondetection by IRAS at the mean orbital distance a_P (not at perihelion). These are runs 1, 2, and 14, with the final distribution being

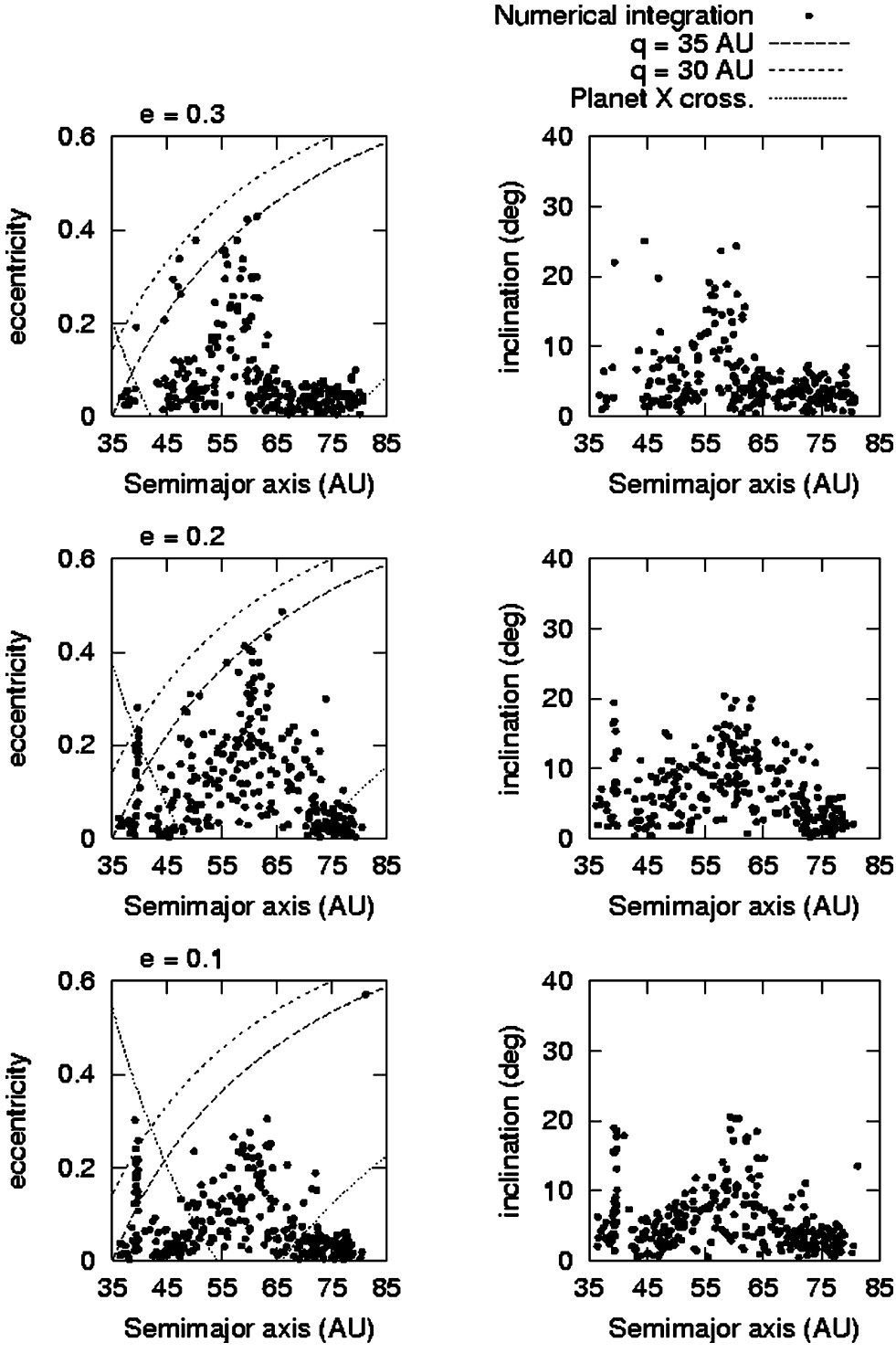

Fig. 2. Final eccentricity and inclination distributions generated in the belt population for different values of the eccentricity, e_P of the hypothetical planet. The mass of the planet is $0.1M_\oplus$ and the initial semimajor axis is $a_P = 60$ AU. These are runs 10, 9, and 8 from Table 1. The lines of representing orbits with perihelion distances of 30 and 35 AU are indicated. Planet X crossing orbits refer to values of the eccentricity such that lines indicating that the aphelion/perihelion of the orbit at the given semimajor axes coincide with the perihelion/aphelion of Planet X.

shown in Fig. 4. There is now clear evidence of bodies being removed from around 50 AU. However none of the final distributions really look like the observed distribution.

We thus conclude that none of parameter sets for Planet X that we have investigated produce a final orbital distribution in the belt that matches observations. Since we have made attempts to investigate the extremes of acceptable parameters for Planet X, we conclude that the Planet X scenario does not work. in some cases the exited state of the belt can be produced, but no gap. In others a

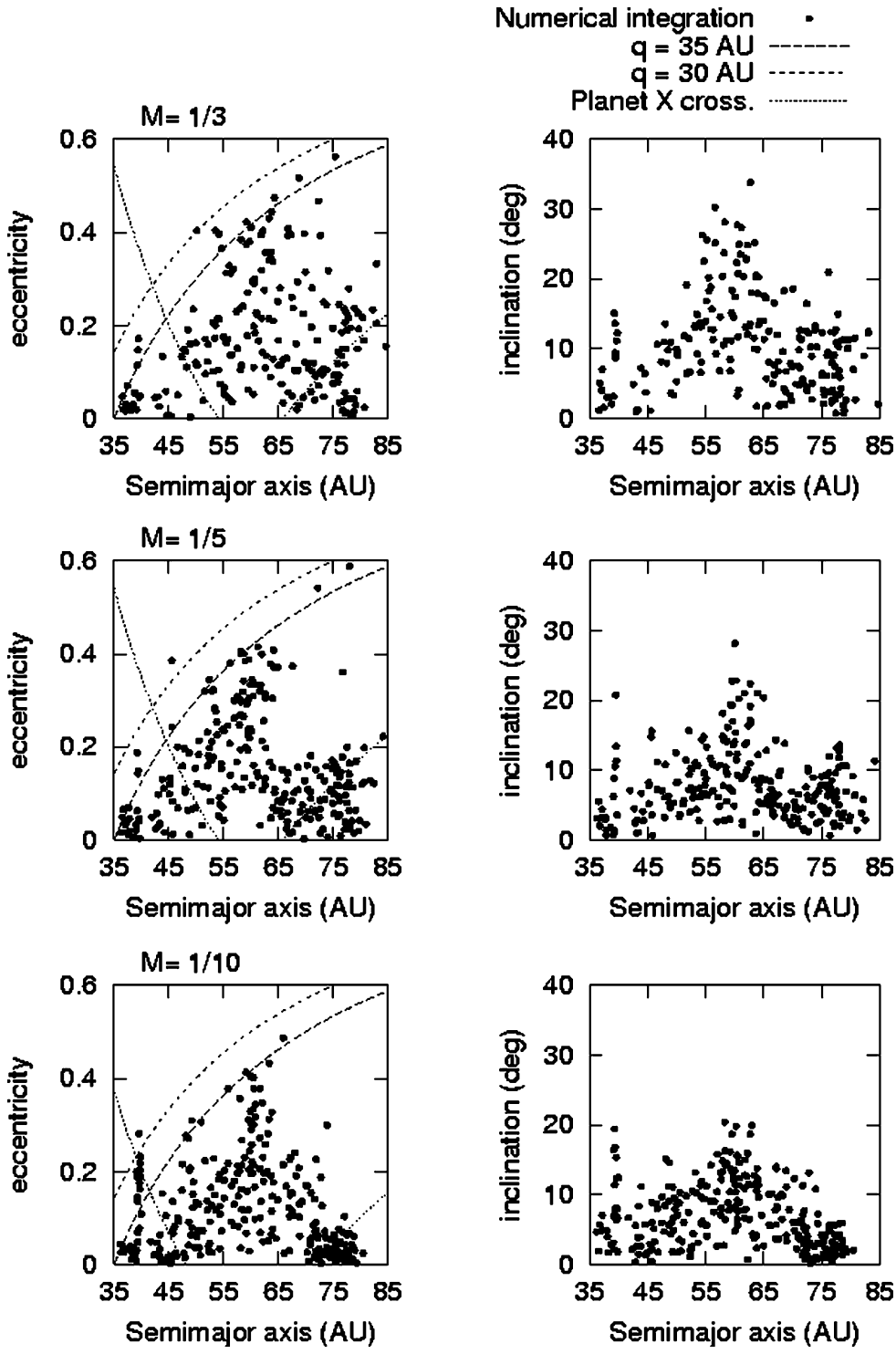

Fig. 3. Final eccentricity and inclination distributions generated in the belt population after 1 Gyr for different values of the mass, m_P of the hypothetical planet. The eccentricity of the planet is $e_P = 0.2$, the inclination $i_P = 10°$ and the initial semimajor axis is $a_P = 60$ AU. These are runs 3, 6, and 9. The lines have the same meaning as in Fig. 2.

gap is formed, but classical belt objects and plutinos are lost.

There is a further difficulty with the Planet X models that have been investigated. The parameter set that gets closest to the observed distribution involves a large planet at a large distance. According to Stern and Colwell (1997b), the accretion of such a big object at those distances is very unlikely. A further problem is that the only effect on Planet X that we have included is the gravitational perturbations of the major planets. The primordial disk that we have considered is in fact far more massive than Planet X. Hence, as Planet X has a gravitational effect on the disk,

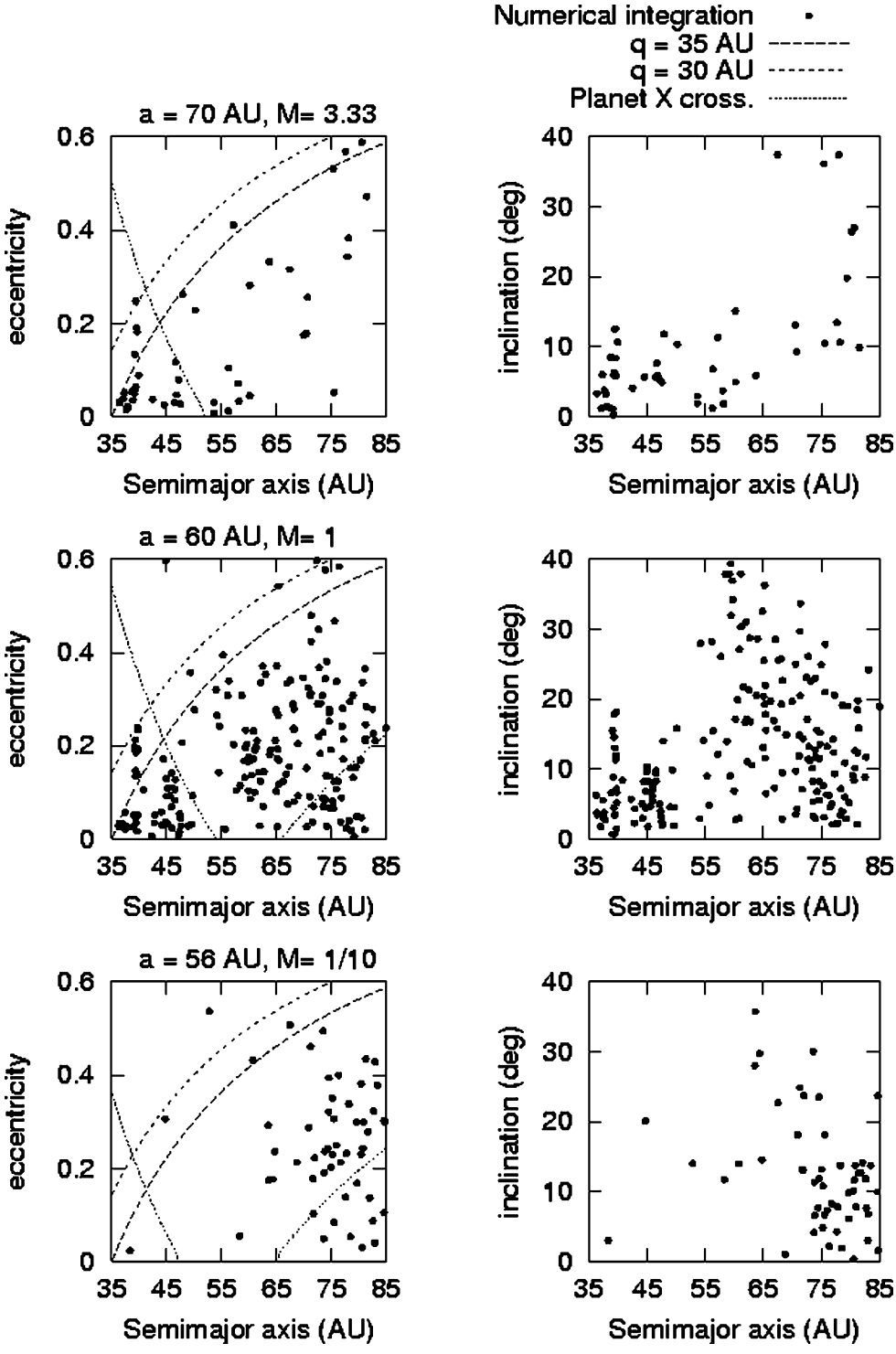

Fig. 4. Final eccentricity and inclination distributions generated in the belt population after 1 Gyr for different orbital and physical parameters of Planet X. The initial perihelion distance in all cases is ∼ 50 AU. These are runs 14, 2, and 1. The lines have the same meaning as in Fig. 2. Masses are in $M_{\oplus}$.

we should expect a corresponding reaction on Planet X. In other words, it is unrealistic to assume that the orbit of Planet X effectively remains with a value of eccentricity close to the initial one throughout the integration interval. We consider these points further in the next section.

5. Evolution of the orbit of a hypothetical Planet X

As we have said, the accretion of a terrestrial-size Planet X at around 60 AU is not very likely (Stern and Colwell, 1997b). A far more likely formation location is the Uranus–Neptune region, with the planet subsequently being

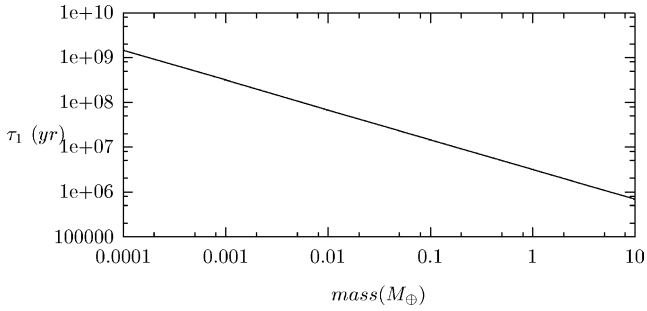

Fig. 5. τ_1 as a function of m_P for a planetoid at $a = 80$ AU and a massive EKB.

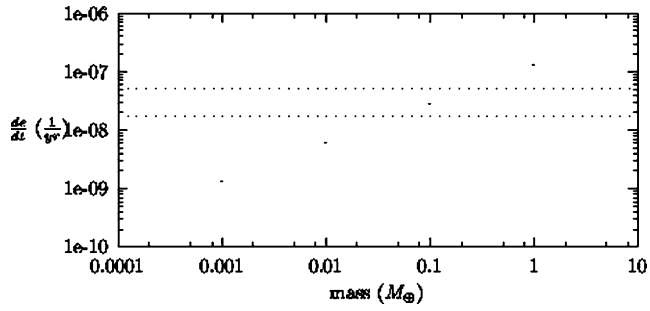

Fig. 6. $(\frac{de_P}{dt})_{\rm DF}$ as a function of m_P. Also shown by the dotted lines are the values of $(\frac{de_P}{dt})_E$ when $a_P = 40$ and 300 AU.

expelled by either Uranus or Neptune after these have already accumulated much of their present mass (Brunini and Melita, 2002). A close encounter with Neptune can not place Planet X on an orbit similar to those investigated, since the point at which the encounter took place must be on both the old and the new orbit. Hence interaction with the primordial Edgeworth–Kuiper belt is essential. We first tackle this problem by semianalytical means and then produce the results of a numerical simulation.

For moderate to large eccentricities the scale of the interaction with the disk is local. In this case, Papaloizou (2002) gives the rate of change of the eccentricity of the planet as:

$$\left(\frac{de_P}{dt}\right)_{\rm DF} = \frac{\pi\Omega\Sigma a_P^3(1.0-e_P^2)^{3/2}m_P}{2R_H e_P^2 M_\odot^2}, \tag{1}$$

where Ω is the mean motion of Planet X, Σ is the surface mass-density of the disk and R_H is local interaction distance, which we take as the Hill radius. We can calculate a time-scale τ_1 for a significant change in eccentricity, (that is $(\Delta e_P)/e_0 \approx 1$)) for any given set of disk parameters and initial Planet X parameters.

Fig. 5 shows τ_1 for a disk of mass $30M_\oplus$ and planet with initial perihelion distance of 35 AU and semimajor axis 80 AU for varying planetary mass m_P.

As can be seen, the time-scale for the orbit of Earth-mass planet to significantly change is less than 10^7 y. Kenyon and Luu (1999) claim that a massive disk is still present at these time-scales, with large Edgeworth–Kuiper objects still forming. This tells us that Planet X can easily escape from the Neptune crossing regime with the available time, but it also says that the orbit will be essentially circular. The data does not tell us the radius of the circular orbit since it deals only with changes in the semimajor axis. Though the time-scales change slightly, the conclusions remain the same for any planet with mass in the range 0.33–$3M_\oplus$.

In order that the planet is decoupled from the control of Neptune, we need to consider the rate of change of eccentricity caused by recurrent close-encounters with Neptune, $(\frac{de_P}{dt})_E$. If this is much greater than the rate of change estimated above, then this effect will dominate. $(\frac{de_P}{dt})_E$ can be estimated as follows. At perihelion, the velocity of the Planet and the kick it receives from Neptune are roughly orthogonal, implying a minimal change in both energy and momentum, hence the perihelion distance q will remain roughly constant. Energy conservation gives

$$\Delta e \approx \frac{GM_{\rm NEP}^2 q}{b^2 V_r^2 M_\odot}, \tag{2}$$

where $M_{\rm NEP}$ is the mass of Neptune, and V_r is the relative velocity at the encounter. We assume that $q \approx 35$ AU and the impact parameter $b \approx 5$ AU is. From this we obtain

$$\left(\frac{de_P}{dt}\right)_E \lesssim \Delta e/T_S, \tag{3}$$

where T_S is the time between encounters with Neptune. We assume that T_S is approximately given by the synodic period of the planet with respect to Neptune. Note that with the Planet at perihelion, the time between encounters can be larger than this, so that our estimation of $(\frac{de_P}{dt})_{\rm DF}$ is an upper limit.

In Fig. 6 we show the values of $(\frac{de_P}{dt})_{\rm DF}$ as a function of m_P. Also shown is the estimated value of $(\frac{de_P}{dt})_E$ for a planet with $a = 40$ AU and $a = 300$ AU. If $m_P > 0.3M_\oplus$, it is apparent that the decoupling is possible for all reasonable values of a_P provided $m_P > 0.3M_\oplus$. Further, if $m_P < 0.05M_\oplus$, there is no reasonable value of a_P so that decoupling can take place. Cometary-sized planetesimals would either be expelled from the Solar System or would still be found only in the Scattered disk. This estimation indicates that objects with large perihelion such as 2000 $\rm CR_{105}$ will not be 'trapped' in the disk. However since we taken an upper limit for $(\frac{de_P}{dt})_{\rm DF}$, the masses that can be captured may be smaller. In reality the behavior is very sensitive to the conditions in the disk and a more detailed numerical study is necessary to explore this. This will be carried out in the next section.

6. A numerical simulation of the orbital evolution

Given sufficient computer power, producing a computer simulation of the whole process, including the effects of a primordial disk, is not difficult. As Figs. 7 and 8 we show the evolution of two hypothetical planets of masses 0.3 and $3M_\oplus$ with semimajor axes at 80 and 62 AU, respectively,

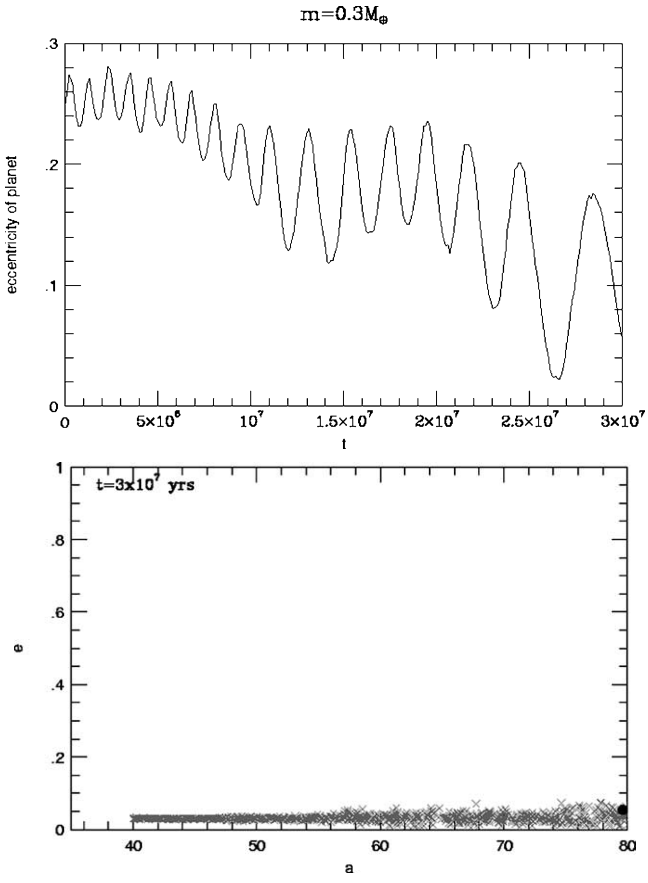

Fig. 7. Eccentricity evolution of a planet of mass $0.3M_{\oplus}$ embedded in a disk of total mass $30M_{\oplus}$.The end-state of the disk after 30 My is also shown.

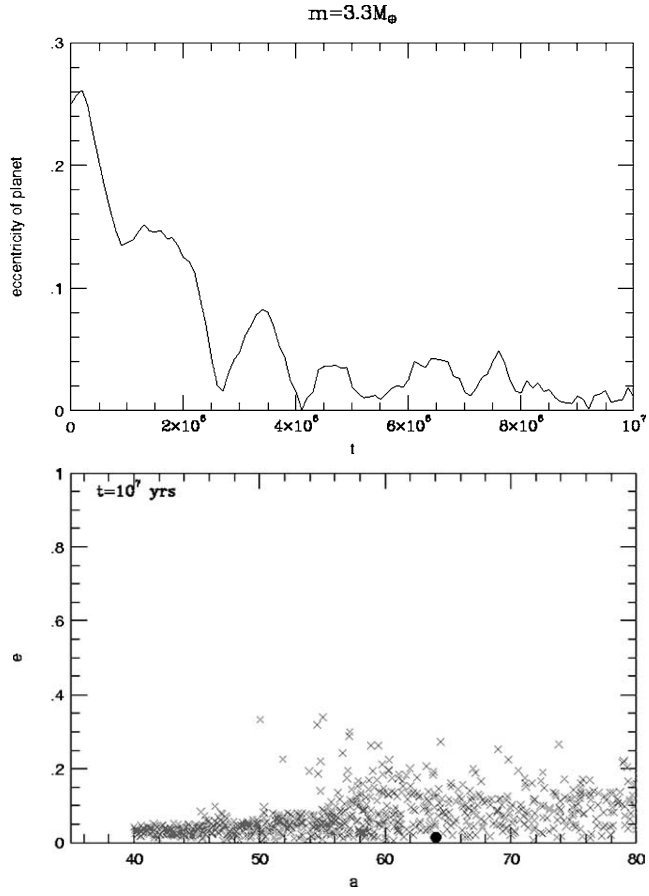

Fig. 8. Eccentricity evolution of a planet of mass $3.3M_{\oplus}$ embedded in a disk of total mass $30M_{\oplus}$. The end-state of the disk after 10 My is also shown.

embedded in a disk of total mass $30M_{\oplus}$ produced by H. Levison (Duncan et al., 1998).

These firmly confirm the conclusions reached in Section 5 above, namely that the orbit of any hypothetical Planet X become circular well within the integration time considered and the semimajor axes do not show any significant evolution. Once this occurs, only a very narrow gap can be swept out, as can be seen.

7. Discussion

In this work we have assessed the possibility of the existence of Planet X, using the known EKBO distribution. Our simulations show that no set of parameters for Planet X can reproduce the observed EKO distribution. There seem to be only two outcomes, either a gap is not cleared, or the process removes large numbers of plutinos and classical belt objects as well as generating a gap.

A discussion of the evolution of the orbit of Planet X also shows that it is not possible for the planet to be on an eccentric orbit at the distances investigated. Indeed the orbital distribution of the Scatter disk as we observe is not consistent with the existence of Planet X (Melita and Williams, 2004).

Given these conclusions, observational detection of a continuation of the Classical EKB beyond 80 AU would lead to an interesting dynamical problem. Similarly, the discovery of a real Planet X would imply a greater primordial number of plutinos. This would add considerable strength to the resonance capture and outward planetary migration proposed by Malhotra (1995).

Acknowledgments

S.J.C.-B. and M.D.M. would like to acknowledge PPARC for providing the funding that enabled this work to be carried out. We are also grateful to J. Papaloizou for useful discussions. We also wish to thank J.M. Pettit for useful comments and Hal Levison for both comments and for running two numerical simulations for us.

References

Allen, R.L., Bernstein, G.M., Malhotra, R., 2001. The edge of the Solar System. Astrophys. J. 549 (2), 241–244.

Brunini, A., Melita, M.D., 2002. The existence of a planet beyond 50 AU and the orbital distribution of the classical Edgeworth–Kuiper-belt objects. Icarus 160, 32–43.

Chambers, J.E., 1999. A hybrid symplectic integrator that permits close encounters between massive bodies. Mon. Not. R. Astron. Soc. 304, 793–799.

Collander-Brown, S.J., Fitzsimmons, A., Fletcher, E., Irwin, M.J., Williams, I.P., 2001. The scattered trans-neptunian objects 1998 XY95. Mon. Not. R. Astron. Soc. 325, 972–978.

Duncan, M., Quinn, T., Tremaine, S., 1989. The long-term evolution of orbits in the Solar System—a mapping approach. Icarus 82, 402–418.

Duncan, M.J., Levison, H.F., 1997. A scattered comet disk and the origin of Jupiter family comet. Science 276, 1670–1672.

Duncan, M.J., Levison, H.F., Budd, S.M., 1995. The dynamical structure of the Kuiper belt. Astron. J. 110, 3073.

Duncan, M.J., Levison, H.F., Lee, M.H., 1998. A multiple time step symplectic algorithm for integrating close encounters. Astron. J. 116 (4), 2067–2077.

Gladman, B., Holman, M., Grav, T., Kavelaars, J.J., Nicholson, P.D., Aksnes, K., Petit, M.J., 2001. Evidence for an extended scattered disk. Icarus 157 (2), 269–279.

Gomes, R., 2003. The origin of the Kuiper belt high-inclination population. Icarus 161, 404–418.

Hogg, D.W., Quinlan, G.D., Tremaine, S., 1991. Dynamical limits on dark mass in the outer Solar System. Astron. J. 101, 2274–2286.

Ida, S., Larwood, J., Burkett, A., 2000. Evidence for early stellar encounters in the orbital distribution of Edgeworth–Kuiper belt objects. Astrophys. J. 528, 531–536.

Jewitt, D., Luu, J., 1993. Discovery of the candidate Kuiper belt object 199 2 QB1. Nature 362, 730–732.

Kenyon, S.J., Luu, J.X., 1999. Accretion in the early Kuiper belt: II. Fragmentation. Astron. J. 118, 1101–1119.

Knezévic, Z., Milani, A., Farinella, P., Froeschlé, Ch., Froeschlé, C., 1991. Secular resonances from 2 to 50 AU. Icarus 93, 316–330.

Kobayashi, H., Ida, S., Tanaka, H., 2004. The evidence of an early stellar encounter in the Edgeworth–Kuiper belt. Icarus. Submitted for publication.

Levison, H.F., Duncan, M.J., 1997. From the Kuiper belt to Jupiter-family comets: the spatial distribution of ecliptic comets. Icarus 127 (1), 13–32.

Levison, H., Morbidelli, A., 2003. The formation of the Kuiper belt by the outward transport of bodies during Neptune's migration. Nature 426, 419–421.

Malhotra, R., 1995. The origin of Pluto's orbit: implications for the Solar System beyond Neptune. Astron. J. 310, 420–429.

Melita, M.D., Brunini, A., 2000. Comparative study of mean-motion resonances in the trans-neptunian region. Icarus 147, 231–245.

Melita, M.D., Williams, I.P., 2004. Planet X and the scattered disk. In: Davis, J. (Ed.), Earth, Moon and Planets, Proceedings of the First Decadal Review of the Edgeworth–Kuiper Belt, ESO International Workshop. In press.

Melita, M.D., Williams, I.P., Larwood, J., Orbital excitation in the Edgeworth–Kuiper belt: the close stellar passage scenario. Icarus. Submitted for publication.

Morbidelli, A., Valsechi, G.B., 1997. Neptune scattered planetesimals could have sculptured the primordial Edgeworth–Kuiper belt. Icarus 128, 464–468.

Nagasawa, M., Ida, S., 2000. Sweeping secular resonances in the Kuiper belt caused by depletion of the solar nebula. Astron. J. 120 (6), 3311–3322.

Papaloizou, J., 2002. Global $m = 1$ modes and migration of protoplanetary cores in eccentric protoplanetary disks. Astron. Astrophys. 388, 615–631.

Stern, S.A., Colwell, J.E., 1997a. Collisional erosion in the primordial Edgeworth–Kuiper and the generation of the 30–50 AU Kuiper gap. Astrophys. J. 490, 879–882.

Stern, S.A., Colwell, J.E., 1997b. Accretion in the Edgeworth–Kuiper belt: forming 100–1000 km radius bodies at 30 AU and beyond. Astron. J. 11, 841.

Trujillo, C.A., Brown, E., 2001. The radial distribution of the Kuiper belt. Astrophys J. 554 (1), 95–98.

Trujillo, C.A., Jewitt, D.C., Luu, J.X., 2001. Properties of the trans-neptunian belt: statistics from the Canada–France–Hawaii Telescope Survey. Icarus 122 (1), 457–473.